



Reconstruction of late Holocene palaeoenvironmental and palaeohydrological changes using multi-proxy analysis of Sattal lake sediments, Kumaun lesser Himalaya, India

Pooja Chand ^{a,*}, Bahadur Singh Kotlia ^{a,1}, David F. Porinchu ^b, Anupam Sharma ^c, Pankaj Kumar ^d, Harish Bisht ^{a,e}, G.C. Kothyari ^f, Manmohan Kukreti ^a

^a Centre of Advanced Study in Geology, Kumaun University, Nainital, Uttarakhand, 263002, India

^b Department of Geography, University of Georgia, Athens, GA, 30602, USA

^c Birbal Sahni Institute of Palaeosciences, 53 University Road, Lucknow, Uttar Pradesh, 226007, India

^d Inter-University Accelerator Center, New Delhi, 110067, India

^e Geology and Mining Department, Champawat, Uttarakhand, 262523, India

^f University of Petroleum and Energy Studies, Dehradun, 248007, India

ARTICLE INFO

Keywords:

Kumaun lesser himalaya
Sattal lake
Late holocene
Medieval climatic anomaly (MCA)
Little ice age (LIA)
Modern warming

ABSTRACT

The present study aims to investigate the palaeoenvironmental changes around Sattal Lake, Kumaun Lesser Himalaya spanning the last 1670 years. Based on multi proxy analysis (i.e., grain size, mineral magnetism, clay mineralogy, Total Organic Carbon (TOC) and carbon isotopes), supported by a robust radiocarbon chronology, three major environmental phases were identified. Warm, wet phases occurred between 1,150–650 cal yr BP and 260 cal yr BP to the present. These phases coincide closely with the Medieval Climatic Anomaly (MCA) and modern warming, respectively. These warm/wet events were due to elevated precipitation, resulting in high lake levels and an expansion of the lake margin, which were marked by lower $\delta^{13}\text{C}$ values, comparatively higher sand concentration, TOC values and magnetic susceptibility (χ_{lf}). The inference of a modern warm phase is supported by high resolution instrumental data. The MCA, which is marked by elevated amounts of coarse grained (sand) detrital material, is inferred to be an interval of strengthened of monsoonal intensity, which correlates with available monsoon records from various continental paleoclimate archives. Following the MCA a cold and dry phase was observed to occur between 610 and 260 cal yr BP, corresponding to the Little Ice Age (LIA). The LIA, which was characterized by high silt and clay concentration, high $\delta^{13}\text{C}$, low TOC and reduced magnetic susceptibility (χ_{lf}), is inferred to represent an interval of low lake levels, likely reflecting an episode of weakened monsoonal intensity.

1. Introduction

Palaeoclimate research plays a major role for better understanding of past climatic variability on longer time spans. The Indian subcontinent is one of the largest monsoon dominated regions on Earth. The climate of Indian Himalayan region, particularly in the Kumaun Lesser Himalaya, is mainly controlled by the Indian Summer Monsoon (ISM)/SW monsoon, Western Disturbances and the NE monsoon (Kotlia et al., 2012; Joshi et al., 2017; Venkateshwarlu et al., 2023). The ISM is a

major component of the regional system, which in turn, is important for the large population of South Asia and variability in the ISM's intensity has had a profound impact on the socioeconomic condition of this region through time (Mishra et al., 2013). It is one of the major sources of fresh water for the peoples of Indian subcontinent (Reddy and Gandhi, 2022). In addition, the rise and demise of civilizations, migration of peoples, beginning of agriculture and development of urban settlements have all been directly or indirectly related to fluctuations in the ISM and associated climate conditions (Kathayat et al., 2017). It is therefore

* Corresponding author.

E-mail addresses: poojachand10june@gmail.com (P. Chand), bahadur.kotlia@gmail.com (B.S. Kotlia), porinchu@uga.edu (D.F. Porinchu), anupam.sharma@bsip.res.in (A. Sharma), baghelnakaj@gmail.com (P. Kumar), harishbisht890@gmail.com (H. Bisht), girishkothyari@gmail.com (G.C. Kothyari), manmohankukreti12@gmail.com (M. Kukreti).

¹ Bahadur Singh Kotlia (deceased).

important to use palaeoclimatic data to investigate the variability of the monsoon system over longer time scales such as the Quaternary (Thompson et al., 1997; Fleitmann et al., 2003).

Paleoclimate records developed in India, including lacustrine (Kotlia et al., 2010; Veena et al., 2014; Phartiyal et al., 2020; Niederman et al., 2021), loess (Dar et al., 2015; Lone et al., 2022), peat bogs (Phadtare, 2000; Rühland et al., 2006; Bhattacharya et al., 2021), speleothems (Sinha et al., 2011; Kotlia et al., 2015), tree rings (Yadav et al., 2014; Shah et al., 2018), glacier (Benn and Owen, 1998; Kumar et al. 2008; Bolch et al., 2012; Bisht et al., 2020) and marine archives (Gupta et al., 2003; Balaji, 2022) have been used to document climatic variability during late Holocene in different parts of the Indian subcontinent. These palaeoclimate records are important for refining global and regional climate models which are being used to help anticipate the future climate conditions. Geochemical traces preserved in sediment records can be used to decipher palaeoenvironmental and palaeoecological histories (Meyers and Teranes, 2001). The chemical and physical characteristics of lake sediment, loess, peat bogs, speleothems and ocean sediments can serve as potential proxies providing crucial information

on climatic fluctuations during the late Quaternary.

Lake sediment deposits are one of the major continental archives used to study past climatic fluctuations as variations in palaeohydrology are reflected in the geochemical, physical and biological properties preserved within these lacustrine sediment records (Mishra, 2014). Extant lakes are ideal for studying the traces of monsoonal fluctuation and climate change in the past. Freshwater lakes in the Himalayan region are structurally controlled closed basins that serve as major sinks for sediment deposition, carbon sequestration, as well as record signatures of past climatic conditions (Mishra, 2014). The lakes present in this region are subject to internal and external pressures, such as tectonic, climatic and geomorphic activity and strongly influenced by both natural and anthropogenic forces (Kotlia and Joshi, 2013). Multi-proxy analysis of lake sediments is helpful for reconstructing palaeoenvironmental and palaeomonsoonal changes by providing climatic records spanning the late Holocene at a decadal-to-centennial-scale resolution.

Here, we reconstruct late Holocene palaeoenvironmental and palaeohydrological changes in Kumaun Lesser Himalaya using multi-proxy

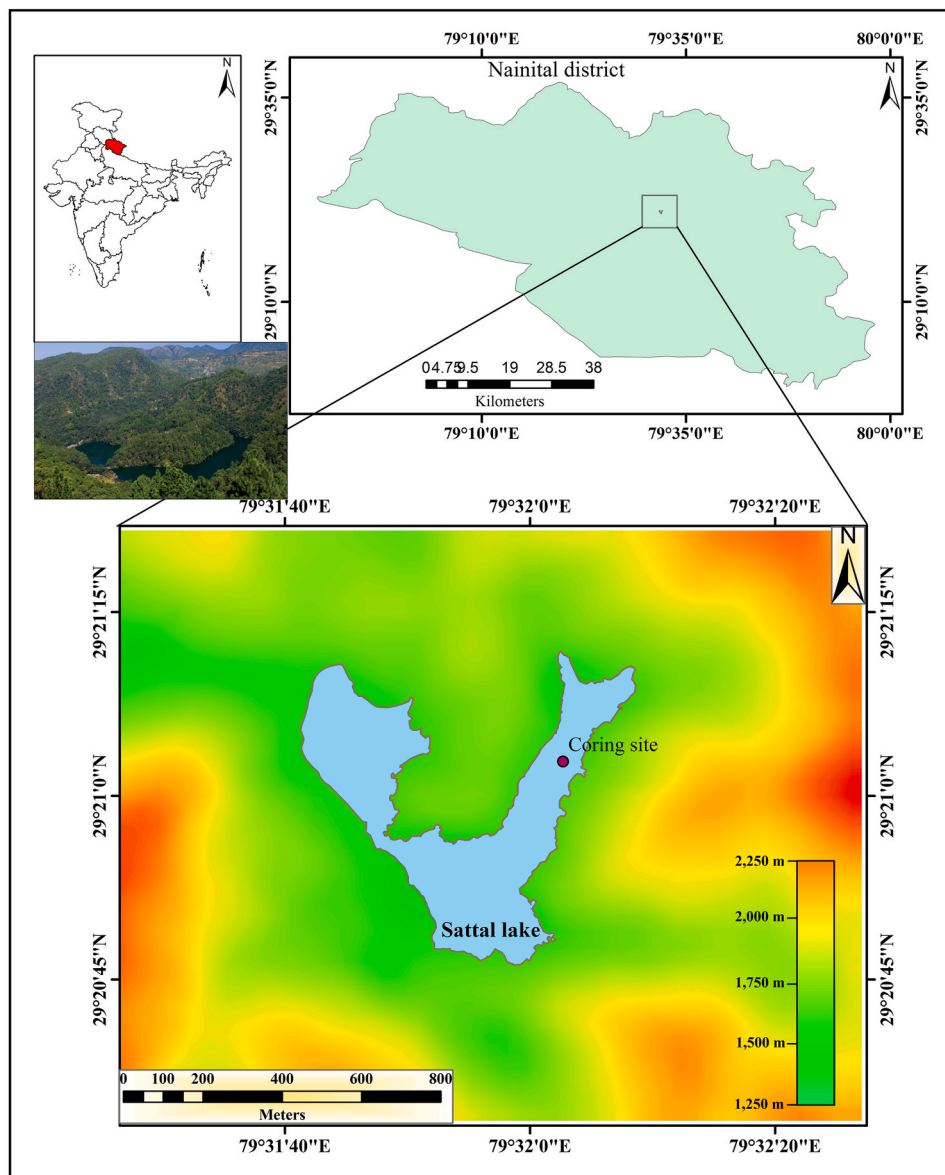


Fig. 1. Location map of the study area with coring site in Sattal Lake, Uttarakhand, India. (noted in red in inset map). (For interpretation of the references to colour in this figure legend, the reader is referred to the Web version of this article.)

analysis of carbon isotopes ($\delta^{13}\text{C}$), grain size, mineral magnetism, total organic carbon (TOC) and clay mineralogy from a lake core retrieved from the Sattal Lake, Uttarakhand. We also compare our reconstructed palaeoclimatic record with the other local and regional paleoclimate records to develop a better understanding of the palaeoclimate conditions that characterized this region during the last two millennia.

2. Study area

Sattal Lake ($29^{\circ} 20' 54.51''\text{N}$, $79^{\circ} 31' 54.77''\text{E}$; 1300 m asl) is an interconnected group of seven fresh water bodies situated in the Nainital district of Uttarakhand, India (Fig. 1). It is a relatively large lake, covering an area of 0.19 km^2 with a maximum width of 0.27 km and length of 0.74 km, with a depth that varies from 1.00 m to 14.38 m. Geologically the area is comprised of mainly the Nagthat, Blaini, Siwalik and Ramgarh formations with Sattal Lake situated in Nagthat Formation (Valdiya, 1980). The Main Boundary Thrust (MBT) and Ramgarh Thrust (RT) are observed in the study region (Fig. 2). The lake is structurally controlled and the catchment comprised chiefly of slate, quartzite, schist and sandstone associated with the above mentioned formations (Valdiya, 1980). This lake is a suitable site for preserving past climate records because it is a closed basin surrounded by dense forest with no outlet, thus, leading to the lake being the main sediment depocenter. Presently, the lake has no active inlet or river channel. The lake is mainly fed by the surface runoff during monsoon season with lesser amounts of freshwater contributed by groundwater. The undisturbed nature of sediment accumulation supports using temporal changes in different proxies (i.e. sediment texture, mineral magnetism, stable isotopes and sediment geochemistry) as a direct measure of the variability in the intensity of the ISM. Similar to other places in the Himalayan region, Sattal experiences a mild climate throughout the year (Harris et al. 2020). The instrumental data for last 120 years are shown in Fig. 3 (see Harris et al., 2020).

In general, the Indian summer monsoon contributes ~85% of total average annual precipitation with the remainder of precipitation associated with western Disturbances (Bustamante et al., 2016). The rainfall data indicate that average annual precipitation between 1901 and 2020 CE varied between 70.50 and 185.11 mm/yr (Fig. 3a). The temperature

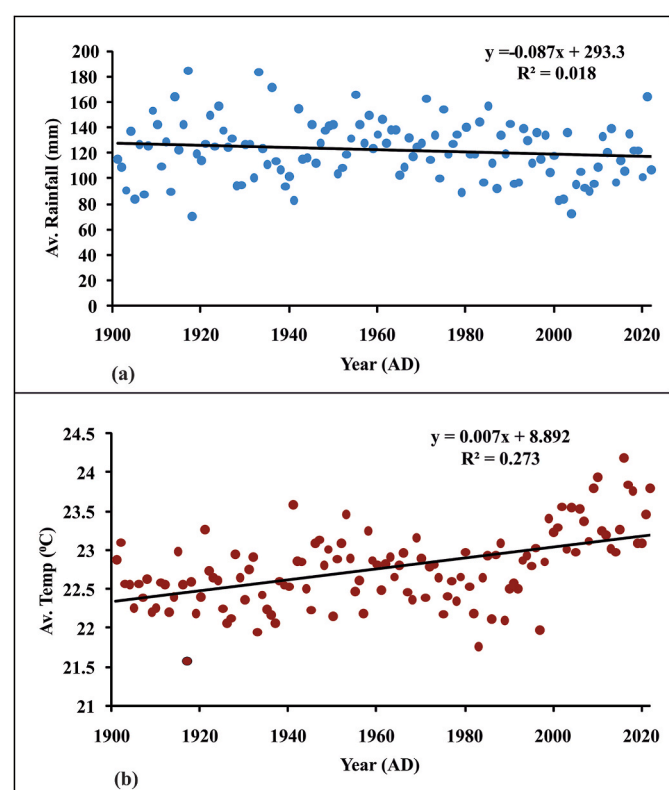


Fig. 3. A graph showing fluctuating trend of the meteorological parameters (a) average annual rainfall, (b) average annual temperature, during last 120 years from 1901 to 2020 (data downloaded from CRUTS 4.7).

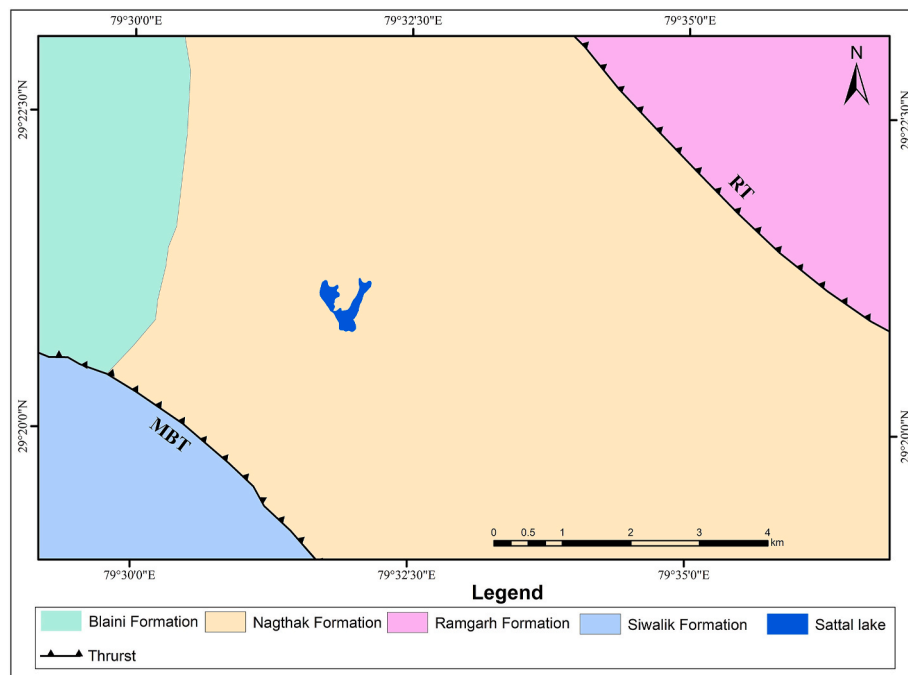


Fig. 2. Regional geological map of the study area (Modified after Valdiya, 1980). MBT: Main Boundary Thrust, RT: Ramgarh Thrust.

data for this same interval indicate that mean annual temperature varies between 2 °C and 27 °C (Fig. 3b).

3. Materials and methods

3.1. Sample collection and preparation

During the fieldwork in June 2018, a 42 cm sediment core was retrieved from the deepest part (29° 21' 02.8" N: 79° 32' 02.7" E; water depth 14.38 m) of Sattal lake by using a gravity piston corer with 7.62 cm diameter. The core was lithologically described using sediment texture/structure and Munsell colour and with light and dark colored minerals and organic rich layers noted. The core was sub-sampled at 0.5 cm resolution; however, the volume of sediment available at this resolution was not sufficient to analyze the full suite of proxies. Merged samples were analyzed at 1 cm intervals for mineral magnetism, 2 cm intervals for carbon isotopes and TOC and 3 cm intervals for grain size and X-ray diffraction analysis. The sub-samples were air dried and packed in a zip lock plastic bags and stored for further analytical processes. Three organically rich bulk sediment samples were selected for AMS ^{14}C dating. A total of 21 samples were analyzed for isotopic analysis and the same samples were also used for the analysis of Total Organic Carbon (TOC) by using an Isotopic Ratio Mass Spectrometer (IRMS). A total of 36 samples were selected for environmental magnetic analysis. Fifteen samples were used for grain size analysis using a particle size analyzer and the same samples were also used for clay mineralogy using X-ray diffraction.

3.2. AMS ^{14}C dating

Three bulk sediment samples were analyzed for ^{14}C at the Inter University Accelerator Center (IUAC), New Delhi. Several plant roots and other organic material such as woods, leaves, etc. were present at the top of the core. Therefore, the sediment samples were assessed visually by using a microscope and potentially problematic organic materials were removed. Approximately 5–10 g of bulk sediment was transferred into a 50 ml centrifuge tube, followed by an Acid-Base-Acid (ABA) treatment using 1 M HCl and 0.1 N NaOH solutions. Further, the samples were centrifuged several times and rinsed, cleaned and neutralized with Milli-Q water. Following neutralizing, the samples were dried and a known amount of was placed in tin capsules and combusted at 950 °C in an element analyzer. The graphitization of the samples was done at 550 °C by graphitizing reaction using Fe as a catalyst and intake of He. The ^{14}C measurements of graphitized samples were carried out using AMS based on a 500kV Pelletron accelerator. The

generated ages were calibrated using IntCal 20 in OxCal ver. 4.4. Finally, an age-depth model was prepared by using linear interpolation method (Fig. 4).

3.3. Environmental magnetism

Variations in environmental magnetism are used for inferring palaeoclimate changes (Maher et al., 1994). Thirty-six samples were analyzed following standard procedures (King and Channell, 1991) at the Paleomagnetic Laboratory of Research School of Earth Sciences, Australian National University (ANU), Canberra. The samples were air dried and tightly packed in a 2 cm³ nonmagnetic plastic containers for magnetic analysis. The magnetic susceptibility (χ_f) was analyzed using AGICO MFK-1 Kappa Bridge with low frequency (0.46 kHz), which shows the concentration of magnetic minerals in the sample.

3.4. Stable carbon isotopes and TOC

A total of 21 samples were analyzed for stable carbon isotopes ($\delta^{13}\text{C}$) and TOC, following standard procedures (Agrawal et al., 2015), at the geochemical laboratory of the Birbal Sahni Institute of Palaeosciences, Lucknow. For $\delta^{13}\text{C}$ analysis, 1 g of bulk sediment sample was transferred into a centrifuge tube and treated with 5% HCl in a hot water bath at 50 °C for 1 h to remove carbonate, and this process was repeated thrice for each sample. Further, the samples were centrifuged with Milli-Q water by using a centrifuge machine at 3000 rpm to remove soluble salts and acids and dried in an oven at 45 °C. The dried samples were pulverized in an agate mortar and filled into the tin capsules for further analysis. An auto sampler was used to feed the tin capsules into the Elemental Analyzer (Flash EA, 2000 HT). During combustion of the samples, CO₂ gas was injected into the Continuous Flow Isotope Ratio Mass Spectrometer (CRIRMS, MAT 253) connected with a Con-Flow IV interface for isotopic analysis. The TOC was determined by the peak area generated through addition of the integrated m/z 44, 45 and 46 signals noticed in the CF-IRMS.

3.5. Sediment texture and XRD analysis

A total of 15 samples were analyzed for sediment texture and using XRD at geochemical laboratory of Birbal Sahni Institute of Paleosciences, Lucknow by using laser particle size analyzer and X-Ray diffractometer, respectively. To prepare samples for granulometric analysis, visible plant material was removed, and to remove carbonate, organic carbon and other contamination, the samples were treated with several chemicals including 136 g of sodium acetate, 88 g of sodium citrate, and 84 g of sodium bicarbonate solution/liter. After each chemical treatment, the samples were rinsed with Milli-Q water, centrifuged and then decanted three times (Knuze, 1965). A Malvern Mastersizer2000 was used to analyze the sand, silt and clay fractions. Further, the output data was processed by Gradistat software (Blott and Pye, 2001) to obtain different sediment parameters.

For separation of clay, 45 ml of Milli-Q water was added and well mixed with the initially processed samples and kept in a centrifuge tube on a stable base for about 7 hr. The uppermost 15 ml of water was decanted into a centrifuge tube and centrifuged for 10 min at 3000 rpm. The clays, thus separated, were mounted on a glass slide as oriented aggregates for preparing clay slides, which was further used for mineralogical study by X-ray diffractometer with PANalytical Pro and Cu-K α radiation on the 2 \AA fraction (Liu et al., 2004).

4. Results and discussion

4.1. Chronology

The chronology of the Sattal Lake sediment core is based on three AMS ^{14}C dates obtained on bulk sediment samples at depths of 41 cm,

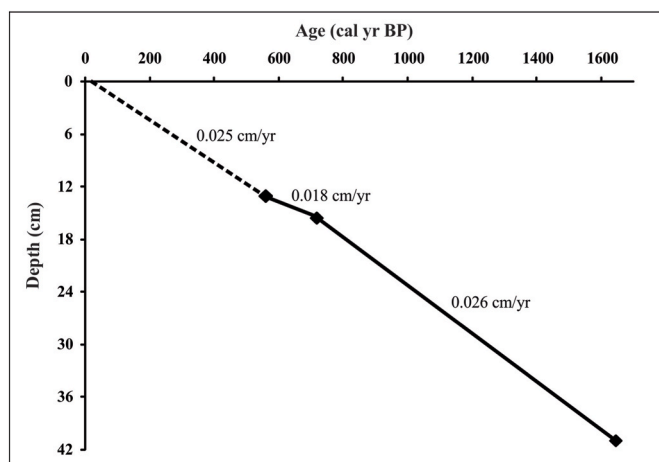


Fig. 4. Age depth model illustrate $^{14}\text{CAMS}$ dates for the Sattal Lake sediment core with the rate of sedimentation estimated for specific intervals.

Table 1The ^{14}C AMS dates obtained for the Sattal Lake sediment core.

Sample No.	IUAC Lab ID	Depth (cm)	^{14}C age (yr BP)	Calibrated age 2- σ (cal. yr BP)	Weighted mean of calibrated age (yr BP)
STL-13	IUACD#5119	13	503 ± 23	551–505	529
STL-16	IUACD#5120	16	808 ± 23	732–676	700
STL-41	IUACD#5117	41	1735 ± 25	1706–1550	1644

16 cm and 13 cm (Table 1). An age-depth model developed using these radiocarbon dates was used to establish a chronology for the entire core (Fig. 4). The age-depth model indicates limited change in the sedimentation rate from the base of the core at ~1,670 cal yr BP to the Present. The highest rate of sedimentation, which is 0.026 cm/yr, occurred between 1640 and 700 cal yr BP (41–16 cm). The lowest rate of sediment, which was 0.018 cm/yr occurred between 700 and 530 cal yr BP (16–13 cm). Overall, the sedimentation rate in Sattal Lake varied from 0.018 cm/yr to 0.026 cm/yr with an average rate of about 0.022 cm/yr. A similar rate of sedimentation characterizes various lakes in India, e.g. 0.055 and 0.077 cm/yr in Kumaun Himalaya (Kusumgar et al., 1989), 0.047 cm/yr in Higher Central Himalaya (Bhushan et al., 2017), 0.019 cm/yr in Karnataka (Sandeep et al., 2017), 0.031 cm/yr in Kerala (Veena et al., 2014), 0.029 cm/yr in Kashmir (Babeesh et al., 2019), 0.039 cm/yr in Rajasthan and 0.029 cm/yr in Tamil Nadu (Sekar et al., 2005).

4.2. Palaeoenvironmental proxies

Considering the age-depth model and successive changes in multi proxy parameters, such as $\delta^{13}\text{C}$, TOC, χ_{lf} , sediment texture and clay mineralogy, the complete profile of the sediment core has been divided into four different climatic zones and is discussed as below.

4.2.1. Sediment texture

Grain size distribution in lake sediment serves as a crucial proxy to comprehend the transport energy, lake level fluctuation and provenance (Conroy et al., 2008; Gyantha et al., 2017). Precipitation plays an important role in erosion, transportation and deposition of sediments from the catchment into the lake (Conroy et al., 2008). During high level of precipitation, increased velocity of the transporting medium enhances the influx of coarse sediment into the lake basin. During intervals of lowered precipitation, a greater proportion of fine sediments are carried to the center of the lake due to the decreased velocity and discharge of

streams draining the catchment (Conroy et al., 2008). Hence, we interpret sediment containing a higher proportion of coarse particles to reflect high rainfall; whereas, a larger proportion of fine particles reflects reduced precipitation. The textural analysis demonstrates that the silt, clay and sand size particles are distributed throughout the entire profile of the sediment core. Overall, the concentration of silt is highest, followed by clay and sand (Fig. 5). In Zone STL-I (42–28 cm; 1,670–1,150 cal yr BP), the concentration of silt varies from 75.2 to 77.1%, and clay and sand concentrations vary from 13.8 to 15.2% and 8.8–10.2%, respectively. In Zone STL-II (28–14 cm; 1,150–610 cal yr BP), the fraction of silt varies between 70.1 and 73.4%, and sand and clay fractions vary from 11.8 to 16.6% and 13.3–15.5%, respectively. Zone STL-II is characterized by the highest concentration of sand, while the silt concentration is lowest. In Zone STL-III (14–6 cm; 610–260 cal yr BP) sand concentration (8.9–12.1%) decreases, while the silt fraction (74.4–76.3%) increases relative to the previous zone with the fraction of clay varying between 13.5 and 14.8%. In Zone STL-IV (6–0 cm; 260–10 cal yr BP), the silt fraction varies between 73.4 and 74.6% and clay fraction from 11.1 to 12.8%, while the sand fraction increases to 12.6–15.5%.

4.2.2. Magnetic susceptibility (χ_{lf})

Magnetic minerals are found everywhere and their presence in soil and sediment samples provides a sensitive substrate for recording changes in the environmental condition (Maher et al., 1994). Based on origin, the magnetic minerals derived from catchment areas can be primary or secondary. Primary magnetic minerals are passed down from the original rocks, while secondary magnetic minerals are created during the process of soil formation or pedogenesis. As a result of chemical weathering, the iron present in ferromagnesian minerals is leached out. Under appropriate Eh-pH conditions, the ferrous ions undergo oxidation to produce magnetite (Maher and Thompson, 1995). Magnetite is considered a secondary magnetic mineral and can be considered pedogenic. Rates of pedogenesis are positively correlated with precipitation. Thus, low (high) rainfall would produce low (high) amounts of pedogenic magnetite, which delivered to the lake through erosion and transportation, would result in low (high) magnetic susceptibility (Balsam et al., 2011). Hence, intervals characterized by high magnetic susceptibility (χ_{lf}) values are inferred to reflect phases of elevated erosion and detrital flux driven by high rainfall. The mechanism of sediment transport, deposition, and/or diagenetic responses can all be affected by environmental changes occurring over a variable time intervals (Veresub and Roberts, 1995). Magnetic susceptibility (χ_{lf}) shows the overall concentration of magnetic materials contained in a natural sample (Walden et al., 1999). In the sediment core, the χ_{lf} values ranges from 2.26 to $5.58 \times 10^{-7} \text{ m}^3/\text{kg}$ (Fig. 5). The highest ($5.58 \times 10^{-7} \text{ m}^3/\text{kg}$)

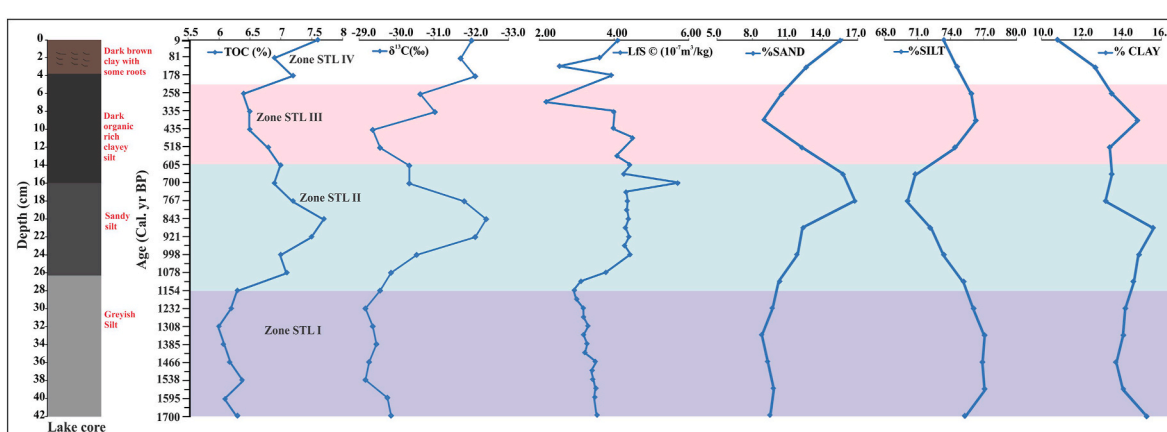


Fig. 5. A multi-proxy record of inferred climatic changes in Sattal Lake, Kumaun Lesser Himalaya based on fluctuations of stable carbon isotopes ($\delta^{13}\text{C}$), TOC (%), magnetic susceptibility (χ_{lf}) and sediment texture. These data are holistically used to divide the record into four zones (STL-I to STL-IV).

and lowest (2.26×10^{-7} m³/kg) values are observed at a depth of 16 cm and 7 cm, respectively. In Zone STL-I, the χ_{lf} values range from 2.98 to 3.54×10^{-7} m³/kg. In Zone STL-II, the χ_{lf} values are increased and range from 3.78 to 5.58×10^{-7} m³/kg. Zone STL-III is characterized by an abrupt decrease in χ_{lf} values (2.26 – 4.46×10^{-7} m³/kg) with the lowest values occurring at 7 cm. In Zone STL-IV, the χ_{lf} values increase with some notable episodes characterized by low χ_{lf} values (2.63×10^{-7} m³/kg).

4.2.3. Stable carbon isotopes ($\delta^{13}\text{C}$)

Stable isotopic studies of lake sediment can provide great insight into lake response to hydroclimate fluctuations (Hammarlund and Buchardt, 1996). The $\delta^{13}\text{C}$ values mainly reflect the organic matter accumulated in the sediment which was carried out into the lake from the catchment (Hillaire et al., 1989; Meyers, 2003). Less negative or richer $\delta^{13}\text{C}$ values suggest a large proportion of C₄ plants with lower precipitation, whereas more negative $\delta^{13}\text{C}$ values indicate a high proportion of C₃ plants with high precipitation (Sandeep et al., 2017). Hence, the variability of $\delta^{13}\text{C}$ value in the lake sediments is inferred to reflect changes in the vegetation cover in the catchment. The $\delta^{13}\text{C}$ values of the lake sediment in entire profile ranges from $-32.4\text{\textperthousand}$ to $-29.1\text{\textperthousand}$ (Fig. 5). The highest value ($-29.1\text{\textperthousand}$) and lowest value ($-32.4\text{\textperthousand}$) recorded at a depth of 30 cm and 20 cm, respectively. In Zone STL-I, the values range from $-29.1\text{\textperthousand}$ to $-29.8\text{\textperthousand}$. In Zone STL-II, an abrupt decrease in the $\delta^{13}\text{C}$ values occurs with the lowest value of $-32.4\text{\textperthousand}$. In Zone STL-III, a gradual increase in the $\delta^{13}\text{C}$ value occurs, with values ranging from $-29.3\text{\textperthousand}$ to $-31.8\text{\textperthousand}$. In Zone STL-IV, the $\delta^{13}\text{C}$ values are characterized by an overall decreasing trend, ranging from $-30.6\text{\textperthousand}$ to $-32.1\text{\textperthousand}$.

4.2.4. Total organic carbon (TOC)

The TOC value of the lake sediment reflects the productivity within the lake and organic input from the surrounding catchment area (Wang et al., 2001; Meyers, 2003). TOC is used as palaeoenvironmental proxy and is mainly influenced by the variables like precipitation, temperature and other lake conditions (Ji et al., 2005; Xu et al., 2006). During hot and humid conditions aquatic and terrestrial plants produce more biomass; whereas, during cold and dry conditions plant growth is reduced due to decreased photosynthesis, resulting in lower primary productivity. Therefore, a higher value of TOC in the lake sediment is

inferred to reflect warm and wet conditions and lower TOC values are inferred to reflect cold, dry conditions (Talbot and Livingstone, 1989). The TOC content of the entire profile varies from 6% to 7.7% (Fig. 5). In Zone STL-I, TOC ranges from 6% to 6.4% with limited variation. In Zone STL-II, TOC gradually increases reaching a peak of 7.7% at 20 cm. Zone STL-III is characterized by an overall decreasing trend with little fluctuation and values varying from 6.4 to 6.8%. Zone STL-IV, is characterized by an overall increasing trend (6.4–7.6%) towards the top of the profile.

4.2.5. Clay mineralogy

Illite is thought to result from the physical weathering of rocks in the dry and cold conditions (Liu et al., 2004). Kaolinite is a secondary mineral derived through the chemical weathering of mica, feldspar, amphibole or pyroxene under warm and humid conditions (Fagel et al., 2003). Chlorite is an alteration product of mafic mineral such as amphibole, pyroxene and biotite, and it is also derived from the weathering and erosion of sedimentary rock under mild conditions (Chamley, 1989). The clay minerals present in Sattal Lake are mainly the product of the physical and chemical weathering of the rocks of different formation (Fig. 2), consisting of sedimentary and metamorphic rocks, that surrounds the lake. The Sattal core is characterized by notable amounts of chlorite, illite and kaolinite. In addition to clay minerals, quartz is also present in the traces associated with illite. A fluctuating trend is observed in the abundance of clay minerals throughout the Sattal profile. Chlorite is the dominant clay mineral, ranging from 40.28 to 43.76% with an average value of 42.18%. Illite and kaolinite range from 27.13 to 34.38% and 10.25–20.28%, respectively (Fig. 6). Quartz + illite vary from 9.39 to 13.65% with an average value of 11.87%. In Zone STL-I, chlorite, illite, kaolinite and illite + quartz range from 41.74 to 42.73%, 30.29–34.38%, 10.25–15.58% and 10.68–13.34%, respectively. In Zone STL-II, an increasing trend is observed in kaolinite, which ranges from 13.28 to 17.8%, and decreasing trend is observed in illite, with its lowest value (27.13%) occurring at 15 cm. Chlorite and quartz + illite show limited variation in this zone. Zone STL-III is characterized by an abrupt decrease in kaolinite with its lowest value (15.14%) occurring at 9 cm. A gradual increase in illite and chlorite (27.13–30.95% and 41.38–43.76%, respectively) occurs in this zone. In Zone STL-IV, a gradual decrease in illite and chlorite (from 29.71 to

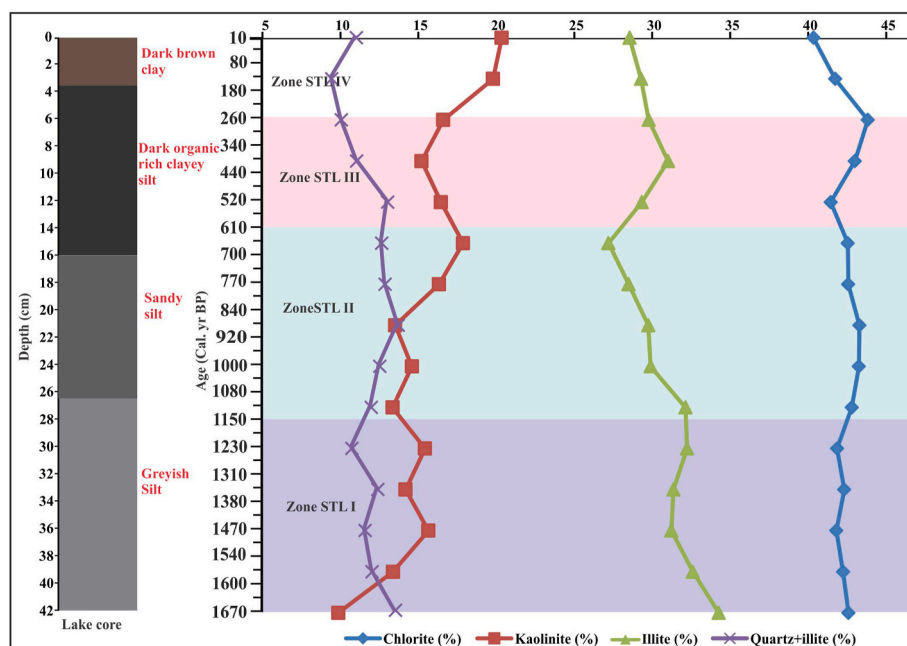


Fig. 6. Variations in the clay mineralogy of the Sattal Lake sediment core.

28.48% and 43.76 to 40.28%, respectively), occurs together with an increase in kaolinite.

5. Palaeoenvironmental reconstruction during the late holocene

The results and inferences derived from the various climatic proxies are used to develop a zonal-based paleoenvironmental reconstruction for the interval captured by the Sattal sediment record.

5.1. Zone STL-I (42–28 cm; 1,670–1,150 cal yr BP)

The sediment texture shows fluctuation in climatic conditions and is characterized by stable magnetic susceptibility (χ_{lf}). A slight decrease in the sand fraction indicates relatively less erosion under dry environment. A decreasing trend of illite supports less weathering under cold and dry climatic conditions while the fluctuating trend of kaolinite indicates a variable climate. The fluctuating concentration of chlorite also supports fluctuating climatic conditions during this interval. The limited variation in TOC and $\delta^{13}\text{C}$ values suggests muted variations in climatic conditions. Based on the multi-proxy analysis, we interpret that this region experienced relatively stable climate conditions between 1,670–1,150 cal yr BP.

5.2. Zone STL-III (28–14 cm; 1,150–610 cal yr BP)

Overall the increase in TOC suggests high productivity within the lake and catchment under warm and wet conditions. The relative decrease in the $\delta^{13}\text{C}$ values also indicates warm and wet conditions during this interval. The gradual increase of sand and overall decrease in silt and clay fractions indicates higher erosion in the catchment mainly due to high rainfall under humid or wet conditions. Such conditions also result in an increase lake volume and lake level due to relatively high rainfall. The elevated average sedimentation rate for this interval (0.026 cm/yr) supports the inference of increased productivity, likely driven by high rainfall as and increased warm condition. The overall increasing trend of χ_{lf} suggests a relatively high detrital influx into the lake from the catchment due to high rainfall under warm and humid conditions. The χ_{lf} values also indicate a close relationship between erosional process and detrital input into the lake basin. Increased kaolinite and decreased illite indicate higher rate of weathering and also suggest a warm/humid climate. Overall, all these inferences, drawn from the different proxy data, point toward the warm and moist conditions and increased monsoon intensity during this time period, which corresponds to the MCA.

5.3. Zone STL-III (14–6 cm; 610–260 cal yr BP)

A gradual decrease in sand concentration indicates less erosion in the catchment due to reduced rainfall, inferred to reflect less humid conditions. Decreasing trend of sand concentration also suggests low lake level. The rising trend of silt and clay fractions indicates low influx from the catchment area, suggesting a low energy depositional environment under dry conditions. A relatively low sedimentation rate (0.023 cm/yr) compared to the Zone STL-II also supports the inference that this zone is characterized by reduced rainfall and dry conditions. The relative increase of $\delta^{13}\text{C}$ suggests the onset of cold and dry conditions with decreasing TOC also supporting this inference. The decrease in TOC driven by reduced autochthonous productivity, is likely a result of moisture limitation of primary productivity. Relative lower values of χ_{lf} further support less detrital input into the lake from the catchment. The increasing trend of illite and decreasing trend of kaolinite indicate reduced rates of weathering and further suggest this interval was characterized by relatively cold and dry conditions. Overall, the multi-proxy analysis suggests that this part of the profile is characterized by cold and dry climatic condition from 610 to 260 cal yr BP which corresponds to the LIA.

5.4. Zone STL-IV (6–0 cm; 260–10 cal yr BP)

Elevated sand concentration indicates this interval was characterized by a high energy depositional environment. The increased sand content also indicates enhanced erosion and higher detrital influx into the lake due to higher precipitation. Hence, the relatively wet climatic conditions and high lake level can be inferred to have existed post-LIA. This zone is characterized by increased TOC and χ_{lf} that indicate a period of higher productivity and intensification of the hydrologic cycle suggesting higher rainfall under warm and humid conditions. The reduced $\delta^{13}\text{C}$ values suggest a relatively high proportion of C_3 plants and high contribution of organic matter into the lake from the catchment due to high rainfall under warm/humid condition. The gradual increase of kaolinite and the decrease in illite as well as chlorite further support the inference of elevated weathering. Overall, the multi-proxy analysis points towards the warm and humid conditions during this period, coinciding with the instrumental data as well, which depicts the trend of rising regional temperature since 1900 AD to present (Fig. 3b).

6. Comparison and correlation with the other palaeoclimatic studies

To better understand monsoon variability during the MCA, LIA and modern warm period in the Kumaun Lesser Himalaya, we have summarized and compared our findings from Sattal Lake with other high resolution palaeoclimatic records from the Indian Himalayan region. The present study shows a strong monsoonal activity and warm and wet conditions in the Kumaun Lesser Himalaya between 1,150–610 cal yr BP. The timing of this warm, wet phase during the late Holocene correlates with regional evidence of the MCA. A warm and wet episode correlative with the timing of the MCA is evidenced in records developed from palaeolakes, modern lakes and cave deposits in the Himalayan region. [Kusumgar et al. \(1995\)](#) reconstructed palaeoclimate using multi-proxy analysis of a lake sediment core recovered from Manasar Lake, Jammu and Kashmir and found that medieval warming started at ~ 900 cal yr BP. On the basis of pollen analysis from Dewar Lake (Garhwal Himalaya), [Chauhan and Sharma \(2000\)](#) documented the existence of a warm, wet phase from 1500 to 900 cal yr BP. A peat bog-based climate reconstruction from Naychudwari Bog (Himachal Pradesh) also suggests that the MCA interval was characterized by warm and wet conditions ([Chauhan, 2006](#)). [Rühland et al. \(2006\)](#) also reported warm and wet conditions in the central Himalaya from 780 cal yr BP onwards. A paleoclimate record, developed based on a sediment core recovered from Demagiri Lake (Mizoram), suggest that the interval between 850 and 400 cal yr BP was characterized by humid conditions ([Mandaokar et al., 2008](#)). A reconstruction of climate variability and palaeovegetation change for Loktak Lake, NE Himalaya revealed warm and humid conditions from 1650 to 600 cal yr BP ([Nautiyal and Chauhan, 2009](#)). Based on the geochemical analysis of Badanital Lake sediments, [Kotlia and Joshi \(2013\)](#) documented that warm and wet conditions, resulting from enhanced monsoon precipitation, occurred between 920 and 440 cal yr BP. Warm and humid conditions were reported from 740 to 590 cal yr BP from Triloknath Glacier, Lahaul Himalaya ([Bali et al., 2017](#)). A warm and wet phase during 1120–760 cal yr BP was reported from a periglacial lake in the Garhwal Himalaya ([Shukla et al., 2020](#)). Multi-proxy analysis of sediment recovered from a proglacial lake in Ladakh, [Phartiyal et al. \(2020\)](#) observed warm conditions from 1270 to 960 cal yr BP. Lastly, [Rawat et al. \(2021\)](#) reported similar findings from Badnikund Lake in Garhwal Himalaya, suggesting a strengthened monsoon and warm conditions existed from 1000 to 700 cal yr BP.

In the Sattal area, cold and dry climatic conditions existed from 610 to 260 cal yr BP, which broadly corresponds to the timing of the LIA. Previous work has identified that this interval was characterized an overall weakening of the monsoon and dry and less humid conditions ([Shukla et al., 2020; Rawat et al., 2021](#)). The cold and dry conditions

between 600 and 500 cal yr BP were reported by [Shah et al. \(2020\)](#) based on a record developed from WularLake, Kashmir. [Shukla et al. \(2020\)](#) studied an exposed section of periglacial lake in the Garhwal Himalaya by using multi-proxy analysis and inferred regional glaciers gained volume and extremely cold conditions existed between ~ 650 and 300 cal yr BP during the LIA when. [Rawat et al. \(2021\)](#) reported similar findings from Badnikund Lake in Garhwal Himalaya, indicating weakening of monsoon and cold climatic condition during the LIA (500-320 cal yr BP). Geochemical proxies from Badanital Lake provide evidence for the expression of the LIA between 440 and 160 cal yr BP in the Garhwal Himalaya. A wet phase between ~ 430 and 170 cal yr BP in the Kumaun Lesser Himalaya, is evidenced in a stalagmite from Chulerasim Cave ([Kotlia et al., 2012](#)). Additional speleothem studies from the region document the existence of cool, wet conditions during the LIA ([Liang et al. 2015; Kotlia et al. 2015](#)). Lastly, [Yadav and Singh \(2002\)](#) reported cool and dry episodes in this region between ~ 420 and 70 cal yr BP. The comparative analysis between the Sattal Lake record and previous studies suggest that resolving the nature of hydroclimate variability in the northern Indian Himalaya remains an outstanding opportunity, requiring additional research.

The uppermost part of the lake core (6-0 cm; 260-10 cal yr BP) is characterized by warm and humid conditions, corresponding to the modern warm period. [Shah et al. \(2020\)](#) documented the existence of warm, humid conditions in Kashmir Himalaya from the 19th to early 20th century. Consistent with the Sattal Lake record, [Kotlia and Joshi \(2013\)](#) reported modern warming trend from 1840 AD onwards in the Garhwal Himalaya. Lastly, [Mann et al. \(2009\)](#) also reported that the monsoon began to intensify at the beginning of 19th century, coinciding with rising atmospheric temperatures.

7. Conclusion

Based on the multi proxy analysis (i.e. sediment texture, magnetic susceptibility (χ_{lf}), clay mineralogy, carbon isotope ($\delta^{13}\text{C}$) and TOC) supported by a robust radiocarbon chronology, our study captures late Holocene climate and environmental change for Kumaun, Lesser Himalaya. The 42 cm long lake sediment core documents climate and depositional history extending from 1670 cal yr BP to the present. The limited variation in the $\delta^{13}\text{C}$, clay mineralogy, TOC, magnetic susceptibility and sediment texture in the lower part of the profile suggest that relatively stable climate conditions prevailed regionally from 1670 to 1150 cal yr BP. The Sattal Lake record also suggest that the warm and wet phases with varying magnitude prevailed in this region between 1150 and 610 cal yr BP and from 260 cal yr BP to the present, coinciding with the Medieval Climate Anomaly (MCA) and modern warming, respectively. During these warm phases, an increase in lake level, marked by the relative high sand fraction, higher magnetic susceptibility, high TOC and decreasing $\delta^{13}\text{C}$ value, is suggestive of humid conditions and of increased monsoon intensity. An increase in the strength of the ISM likely led to the observed increase in chemical weathering and erosion in the catchment area. Furthermore, the cold and less humid phase that existed between 610 and 260 cal yr BP corresponds to the LIA. Lowered lake levels observed during this interval, suggestive of cold and less humid conditions, likely reflect a weakening of the ISM. Relatively cool, less humid conditions are evidenced by low magnetic susceptibility, high $\delta^{13}\text{C}$ values, low TOC, high clay and silt fractions and high amounts of illite. The results from Sattal Lake are consistent with existing studies in Indian Himalayan region.

Funding

The study was partially funded by Department of Science and Technology, Government of India, New Delhi, through fellowship to PC under DST Inspire Program (No. DST/INSPIRE Fellowship/2018/IF180098). A National Science Foundation Human-Environment and Geographical Sciences Award (GSS-2026311) to D.F.P and B.S.K. and a

U.S. Fulbright-Nehru Fellowship and Global Collaborative Research Grant from the University of Georgia (UGA) to D.F.P. also supported portions of this research.

Author's contribution

All authors contributed to the conception and design of this study. PC, BSK and HB drafted the whole manuscript. Sample collection and sample preparation were performed by PC, BSK, DFP, MK and HB. The samples were analyzed by PC. MK helped in preparing age depth model. AS and PK provided comments to improve the manuscript. All authors reviewed and approved the manuscript before submission.

CRediT authorship contribution statement

Pooja Chand: Writing – original draft, Formal analysis. **Bahadur Singh Kotlia:** Writing – original draft, Conceptualization. **David F. Porinchu:** Writing – review & editing, Conceptualization. **Anupam Sharma:** Methodology. **Pankaj Kumar:** Investigation. **Harish Bisht:** Writing – original draft, Methodology. **G.C. Kothiyari:** Writing – original draft. **Manmohan Kukreti:** Methodology.

Declaration of competing interest

The authors declare that they have no known competing financial interests or personal relationships that could have appeared to influence the work reported in this paper.

Data availability

Data will be made available on request.

Acknowledgements

Authors are thankful to the Head, Department of Geology, Kumaun University, Nainital, for providing necessary working facilities. We express our sincere thanks to the Directors, Birbal Sahni Institute of Palaeosciences, Lucknow and Inter University Accelerator Center, New Delhi, for providing laboratory and analytical facilities. PC is thankful to the ARCH India, AIRS Fellowship Program by which a part of analytical work has been carried out in the Research School of Earth Sciences, Australian National University under the supervision of Dr. Andrew P. Roberts and his research associates including Dr. David Heslop, PengXiang and Yao Qian. We are also thankful to Shahdita Bakshi and Kalpana Gururani for their assistance in the field and laboratory for sample collection and preparation respectively.

References

- Agrawal, S., Srivastava, P., Sonam, Meena, N.K., Rai, S.K., Bhushan, R., Mishra, D.K., Gupta, A.K., 2015. Stable ($\delta^{13}\text{C}$ and $\delta^{15}\text{N}$) isotopes and magnetic susceptibility record of late Holocene climate change from a lake profile of the northeast Himalaya. *J. Geol. Soc. India* 86 (6), 696–705.
- Babeesh, C., Achyuthan, H., Resmi, M.R., Nautiyal, C.M., Shah, R.A., 2019. Late holocene paleoenvironmental changes inferred from Manasbal Lake sediments, Kashmir valley, India. *Quat. Int.* 507, 156–171.
- Balaji, D., 2022. Palaeoclimatic reconstructions based on marine sediments from the northern Indian ocean. Implications to Aeolian Flux and Productivity. Maharaja Sayajirao University of Baroda. Ph.D. Thesis.
- Bali, R., Khan, I., Sangode, S.J., Mishra, A.K., Ali, S.N., Singh, S.K., Tripathi, J.K., Singh, D.S., Srivastava, P., 2017. Mid to late Holocene climate response from the Triloknathpalaeolake, Lahaul Himalaya based on multiproxy data. *Geomorphology* 284, 206–219.
- Balsam, W.L., Ellwood, B.B., Ji, J., Williams, E.R., Long, X., Hassani, A.E., 2011. Magnetic susceptibility as a proxy for rainfall: worldwide data from tropical and temperate climate. *Quat. Sci. Rev.* 30 (20), 2732–2744. <https://doi.org/10.1016/j.quascirev.2011.06.002>.
- Benn, D.I., Owen, L.A., 1998. The role of Indian Summer Monsoon and the mid-latitude westerlies in Himalayan glaciation: review and speculative discussion. *J. Geol. Soc. Lond.* 155, 353–363.

Bhattacharya, S., Kishor, H., Yadav, A., Mishra, P.K., Srivastava, P., 2021. Vegetation history in a peat succession over the past 8,000 years in the ISM-controlled kedarnath region, garhwal Himalaya: reconstruction using molecular fossils. *Front. Earth Sci.* 9 <https://doi.org/10.3389/feart.2021.703362>.

Bhushan, R., Sati, S.P., Rana, N., Shukla, A.D., Mazumdar, A.S., Juyal, N., 2017. High resolution millennial and centennial scale Holocene monsoon variability in the Higher Central Himalayas. *Palaeogeogr. Palaeoclimatol. Palaeoecol.* 489, 95–104.

Bisht, H., Kotlia, B.S., Kumar, K., Joshi, L.M., Sah, S.K., Kukreti, M., 2020. Estimation of the recession rate of Gangotri glacier, Garhwal Himalaya (India) through kinematic GPS survey and satellite data. *Environ. Earth Sci.* 79 (329), 1–14.

Blott, S.J., Pye, K., 2001. GRADSTAT: a grain size distribution and statistics package for the analysis of unconsolidated sediments. *Earth Surf. Process. Landforms* 26, 1237–1248.

Bolch, T., Kulkarni, A., Kabb, A., Huggel, C., Paul, F., Cogley, J.G., Frey, H., Kargel, J.S., Fujita, K., Scheel, M., Bajracharya, S., Stoffel, M., 2012. The state and fate of Himalayan glaciers. *Science* 303 (6766), 310–314.

Bustamante, M.G., Cruz, F.W., Vuille, M., et al., 2016. Holocene changes in monsoon precipitation in the Andes of NE Peru based on $\delta^{18}\text{O}$ speleothem records. *Quat. Sci. Rev.* 146, 274–286. <https://doi.org/10.1016/j.quascirev.2016.05.023>.

Chamley, H., 1989. Clay formation through weathering. *Clay Sedimentol* 21–50.

Chauhan, M.S., 2006. Late Holocene vegetation and climate change in the alpine belt of Himachal Pradesh, India. *Curr. Sci.* 91, 1572–1578.

Chauhan, M.S., Sharma, C., 2000. Late holocene vegetation and climate in dewar tal area, inner lesser garhwal Himalaya. *Palaeobotanist* 49, 509–514.

Conroy, J.L., Overpeck, J.T., Cole, J.E., Shanahan, T.M., Kannan, S., 2008. Holocene changes in eastern tropical Pacific climate inferred from a Galápagos lake sediment record. *Quat. Sci. Rev.* 27, 1166–1180.

Dar, R.A., Chandra, R., Romshoo, S.A., Lone, M.A., Ahmad, S.M., 2015. Isotopic and micro morphological studies of Late Quaternary loess paleosol sequences of the Kareda group: inferences for palaeoclimate of Kashmir valley. *Quat. Int.* 371, 122–134.

Fagel, N., Boski, T., Likhoshway, L., Oberhaensli, H., 2003. Late quaternary clay mineral record in central lake baikal (academician ridge, siberia). *Palaeogeogr. Palaeoclimatol. Palaeoecol.* 193 (1), 159–179.

Fleitmann, D., Burns, S.J., Mudelsee, M., Neff, U., Kramers, J., Mangini, A., Matter, A., 2003. Holocene forcing of the Indian monsoon recorded in a stalagmite from Southern Oman. *Science* 300, 1737–1739.

Gupta, A.K., Anderson, D.M., Overpeck, J.T., 2003. Abrupt changes in the asian southwest monsoon during the holocene and their links to the north atlantic ocean. *Nature* 421, 354–357.

Gyantha, K., Routh, J., Chandrajith, R., 2017. A multi-proxy reconstruction of the late Holocene climate evolution in Lake Bolgoda, Sri Lanka. *Palaeogeogr. Palaeoclimato. Palaeoecol.* 443, 16–25. <https://doi.org/10.1016/j.palaeo.2017.01.049>.

Hammarlund, D., Buchardt, B., 1996. Composite stable isotope records from a late weichselian lacustrine sequence at grønne, lolland, Denmark: evidence of allerød and younger dryas environments. *Boreas* 25 (1), 8–22. <https://doi.org/10.1111/j.1501-3885.1996.tb00831.x>.

Harris, I., Osborn, T.J., Jones, P., Lister, D., 2020. Version 4 of the CRU TS monthly high-resolution gridded multivariate climate dataset. *Sci. Data* 7, 109. <https://doi.org/10.1038/s41597-020-0453-3>.

Hillaire, C., Aucour, A.M., Bonnefille, R., Rirollet, G., Vincens, A., Williamson, D., 1989. ^{13}C /Palynological evidences of differential residence times of organic carbon prior to its sedimentation in East African Rift Lakes and peat bogs. *Quat. Sci. Rev.* 8 (3), 207–212. [https://doi.org/10.1016/0277-3791\(89\)90037-1](https://doi.org/10.1016/0277-3791(89)90037-1).

Ji, S., Xingqi, L., Sumin, W., Matsumoto, R., 2005. Palaeoclimatic changes in the Qinghai Lake area during the last 18,000 years. *Quat. Int.* 136, 131–140.

Joshi, L.M., Kotlia, B.S., Ahmad, S.M., Wu, C.C., Sanwal, J., Raza, W., Singh, A.K., Shen, C.C., Long, T., Sharma, A.K., 2017. Reconstruction of Indian monsoon precipitation variability between 4.0 and 1.6 ka BP using speleothem $\delta^{18}\text{O}$ records from the Central Lesser Himalaya, India. *Arabian J. Geosci.* 356 (10) <https://doi.org/10.1007/s12517-017-3141-7>.

Kathayat, G., Cheng, H., Sinha, A., Yi, L., Li, X., Zhang, H., Li, H., Ning, Y., Edwards, R.L., 2017. The Indian monsoon variability and civilization changes in the Indian subcontinent. *Sci. Adv.* 3 (12), 1–8. <https://doi.org/10.1126/sciadv.1701296>.

King, J.W., Channell, J.E.T., 1991. Sedimentary magnetism, environmental magnetism, and magnetostratigraphy. *Rev. Geophys.* 29, 358–370. <https://doi.org/10.1002/rog.1991.29.s1.358>.

Knuze, G.W., 1965. Pre-treatment for mineralogical analysis. In: *Methods of Soil Analysis. Agronomy: American Society of Agronomy*, 9. American Society of Agronomy Inc, Madison, WI, pp. 568–577.

Kotlia, B.S., Joshi, L.M., 2013. Late holocene climatic changes in garhwal Himalaya. *Curr. Sci.* 104 (7), 911–919.

Kotlia, B.S., Sanwal, J., Phartiyal, B., Joshi, L.M., Trivedi, A., Sharma, C., 2010. Late Quaternary climatic changes in the eastern Kumaun Himalaya, India, as deduced from multi-proxy studies. *Quat. Int.* 213, 44–55. <https://doi.org/10.1016/j.quaint.2009.09.002>.

Kotlia, B.S., Ahmad, S.M., Zhao, J.X., Raza, W., et al., 2012. Climatic fluctuations during the LIA and post-LIA in the Kumaun Lesser Himalaya, India: evidence from a 400 yr old stalagmite record. *Quat. Int.* 263, 129–168.

Kotlia, B.S., Singh, A.K., Joshi, L.M., Dhaila, B.S., 2015. Precipitation variability in the Indian Central Himalaya during last ca. 4,000 years inferred from a speleothem record: impact of Indian Summer Monsoon (ISM) and Westerlies. *Quat. Int.* 371, 244–253.

Kumar, K., Dumka, R.K., Miral, M.S., Satyal, G.S., Pant, M., 2008. Estimation of retreat rate of Gangotri glacier using rapid static and kinematic GPS survey. *Curr. Sci.* 94 (2), 258–262.

Kusumgar, S., Agrawal, D.P., Sharma, P., 1989. Radiocarbon chronology and magnetic susceptibility variation in Kumaon lake sediments. In: Long, A., Kra, R.S., Srdz, D. (Eds.), *Proceedings of the 13th International ^{14}C Conference*, 31. Radiocarbon, pp. 957–964, 3.

Kusumgar, S., Agrawal, D.P., Deshpande, R.D., Sharma, R.C., Yadava, M.G., 1995. A comparative study of monsoonal and nonmonsoonal himalayan lakes, India. In: Coop, G.T., Harkness, D.D., Miller, B.F., Scott, E.M. (Eds.), *Proceedings of the 15th International ^{14}C Conference*, 37. Radiocarbon, pp. 191–195, 2.

Liang, F., Brook, G.A., Kotlia, B.S., Railsback, L.B., Hardt, B., Cheng, H., Edwards, R.L., Kandasamy, S., 2015. Panigarh cave stalagmite evidence of climate change in the Indian Central Himalaya. *Quat. Sci. Rev.* 124 (15), 145–161. <https://doi.org/10.1016/j.quascirev.2015.07.017>.

Liu, Z., Colin, C., Trentesaux, A., Blamart, D., Bassinot, F., Siani, G., Sicre, M.A., 2004. Erosional history of the eastern Tibetan Plateau since 190 kyr ago: clay mineralogical and geochemical investigations from the southwestern South China Sea. *Mar. Geol.* 209 (4), 1–18.

Lone, A.M., Shah, R.A., Achyuthan, H., Ahmad, N., Qasim, A., Tripathy, G.R., Samanta, A., Kumar, P., 2022. The late holocene hydroclimate variability in the northwest Himalaya: sedimentary clues from the wular lake, Kashmir valley. *J. Asian Earth Sci.* 229, 105184.

Maher, B.A., Thompson, R., 1995. Palaeorainfall reconstruction from pedogenic magnetic susceptibility variations in the Chinese loess and paleosols. *Quat. Res.* 44, 383–391.

Maher, B.A., Thompson, R., Zhou, L.P., 1994. Spatial and temporal reconstructions of changes in the Asian palaeomonsoon: a new mineral magnetic approach. *Earth Planet Sci. Lett.* 125, 461–471.

Mandaokar, B.D., Chauhan, M.S., Chatterjee, S., 2008. Fungal remains from late holocene lake deposit of Demagiri, Mizoram, India and their palaeoclhyatic implications. *J. Palaeontol. Soc. India* 53 (1–2), 197.

Mann, M.E., Zhang, Z., Rutherford, S., Bradley, R.S., Hughes, M.K., Shindell, D., Ammann, C., Faluvegi, G., Ni, F., 2009. Global signatures and dynamical origins of the little ice age and medieval climate anomaly. *Science* 326, 1256–1260.

Meyers, P.A., 2003. Applications of organic geochemistry to paleolimnological reconstructions: a summary of examples from the Laurentian Great Lakes. *Org. Geochem.* 34 (2), 261–289.

Meyers, P.A., Teranes, J.L., 2001. Sediment organic matter. In: Last, W.M., Smol, J.P. (Eds.), *Tracking Environmental Change Using Lake Sediments. Develop. in Paleoenviron. Res.* Springer. https://doi.org/10.1007/0-306-47670-3_9.

Dordrecht.

Mishra, P.K., 2014. Late quaternary climate variability in the Indian monsoon domain. *Dissertation Submitted in Fachbereich Geowissenschaften, Freie Universität, Berlin.*

Mishra, P., Praveen K., Anoop, A., Menzel, P., Gaye, B., Basavaiah, N., Jehangir, A., Prasad, S., 2013. Holocene Climatic Variability in the Indian Monsoon Domain. *General Assembly European Geosciences Union, Vienna, Austria, 2013.*

Nautiyal, C.M., Chauhan, M.S., 2009. Late Holocene vegetation and climate change in Loktak Lake region, Manipur, based on pollen and chemical evidence. *Palaeobotanist* 58 (1–3), 21–28.

Niederman, E.A., Porinchu, D.F., Kotlia, B.S., 2021. Hydroclimate change in the Garhwal Himalaya, India at 4200 yr BP coincident with the contraction of the Indus civilization. *Sci. Rep.* 11, 23082 <https://doi.org/10.1038/s41598-021-02496-5>.

Phadtare, N.R., 2000. Sharp decrease in summer monsoon strength 4000–3500 calyr B.P. In the central higher Himalaya of India based on pollen evidence from alpine peat. *Quat. Res.* 53 (1), 122–129. <https://doi.org/10.1006/qres.1999.2108>.

Phadtare, N.R., 2020. Late holocene climatic record from a glacial lake in Ladakh range, trans-himalaya, India. *Holocene* 30 (7), 1029–1042. <https://doi.org/10.1177/0959683620908660>.

Rawat, V., Rawat, S., Srivastava, P., Negi, P.S., Prakasam, M., Kotlia, B.S., 2021. Middle Holocene Indian summer monsoon variability and its impact on cultural changes in the Indian subcontinent. *Quat. Sci. Rev.* 255, 106825 <https://doi.org/10.1016/j.quascirev.2021.106825>.

Reddy, A.P., Gandhi, N., 2022. Indian summer monsoon variability on different timescales and deciphering its oscillations from irregularly spaced paleoclimate data using different spectral techniques. In: Kumar, N., Damodara, P. (Eds.), *Holocene Climate Change and Environment*. Elsevier, pp. 339–368. <https://doi.org/10.1016/B978-0-323-90085-0.00025-5>.

Rühland, K., Phadtare, N.R., Pant, R.K., Sangode, S.J., Smol, J.P., 2006. Accelerated melting of Himalayan snow and ice triggers pronounced changes in a valley peatland from northern India. *Geophys. Res. Lett.* 33 (15) <https://doi.org/10.1029/2006GL026704>.

Shah, S.K., Pandey, U., Mehrotra, N., 2018. Precipitation reconstruction for the lidder valley, Kashmir Himalaya using tree-rings of cedrusdeodara. *Int. J. Climatol.* 38, 758–773.

Sandeep, K., Shankar, R., Warrier, A.K., Yadava, M.G., Ramesh, R., Jani, R.A., Weijian, Z., Xuefeng, Lu., 2017. A multi-proxy lake sediment record of Indian summer monsoon variability during the Holocene in southern India. *Palaeogeogr. Palaeoclimatol. Palaeoecol.* 476, 1–14. <https://doi.org/10.1016/j.palaeo.2017.03.021>.

Sekar, B., Bhattacharyya, A., Bera, S.K., 2005. ^{14}C dating of lake sediments, variation in organic matter content and sedimentation rates in three diverse eco zones in the Indian Subcontinent and their impact on lake succession and past climatic oscillations. *PAGES-OSM, Beijing. Book of Abstracts* 155.

Shah, R.A., Achyuthan, H., Lone, A., Kumar, P., Ali, A., Rahman, A., 2020. Palaeoenvironment shifts during last ~500 years and eutrophic evolution of the wular lake, Kashmir valley, India. *Limnology* 22, 111–120. <https://doi.org/10.1007/s10201-020-00639-7>.

Shukla, T., Mehta, M., Dobhal, D.P., Bohra, A., Pratap, B., Kumar, A., 2020. Late-Holocene climate response and glacial fluctuations revealed by the sediment record of the monsoon-dominated Chorabari Lake, Central Himalaya. *Holocene* 30 (7). <https://doi.org/10.1177/0959683620908654>.

Sinha, A., Berkelhammer, M., Stott, L., Mudelsee, M., Cheng, H., Biswas, J., 2011. The leading mode of Indian Summer Monsoon precipitation variability during the last millennium. *Geophys. Res. Lett.* 38, 15703 <https://doi.org/10.1029/2011GL047713>.

Talbot, M.R., Livingstone, D.A., 1989. Hydrogen index and carbon isotopes of lacustrine organic matter as lake level indicators. *Palaeogeo. Palaeoclimato. Palaeoecol.* 70, 121–137.

Thompson, L.G., Yao, T., Davis, M.E., Henderson, K.A., Mosley-Thompson, E., Lin, P.N., Beer, J., Synder, H.A., Dai, J.C., Bolzan, J.F., 1997. Tropical climate instability: the last glacial cycle from a Qinghai-Tibetan ice core. *Science* 276 (5320), 1821–1825.

Valdiya, K.S., 1980. The two intracrustal boundary thrusts of the Himalaya. *Tectonophysics* 66 (4), 323–348. [https://doi.org/10.1016/0040-1951\(80\)90248-6](https://doi.org/10.1016/0040-1951(80)90248-6).

Veena, M.P., Achyuthan, H., Eastoe, C., Farooqui, A., 2014. A multi-proxy reconstruction of monsoon variability in the late Holocene, South India. *Quat. Int.* 325, 63–73.

Venkateshwarlu, M., Babu, N.R., Kapawar, M.R., Kotlia, B.S., Singh, A.K., Satyakumar, A.V., 2023. Magnetostratigraphy of palaeolake sequence from Kumaun Lesser Himalaya, India: implications on young geomagnetic excursions. *Geol. J.* <https://doi.org/10.1002/gj.4682>.

Verosub, K.L., Roberts, A.P., 1995. Environmental magnetism: past present and future. *J. Geophys. Res.* 100, 2175–2192. <https://doi.org/10.1029/94JB02713>.

Walden, J.F., Oldfield, F., Smith, J., 1999. *Environmental magnetism: a practical guide*, No. 6. Quat. Res. Assoc. London 243.

Wang, X.C., Chen, R.F., Whelan, J., Eglinton, L., 2001. Contribution of “Old” carbon from natural marine hydrocarbon seeps to sedimentary and dissolved organic carbon pools in the Gulf of Mexico. *Geophys. Res. Lett.* 28 (17), 3313–3316. <https://doi.org/10.1029/2001GL013430>.

Xu, H., Ai, L., Tan, L., An, Z., 2006. Stable isotopes in bulk carbonates and organic matter in recent sediments of lake qinghai and their climatic implications. *Chem. Geol.* 235, 262–275.

Yadav, R.R., Singh, J., 2002. Tree-ring-based spring temperature patterns over the past four centuries in Western Himalaya. *Quat. Res.* 57, 299–305.

Yadav, R.R., Mishra, K.G., Kotlia, B.S., Upreti, N., 2014. Premonsoon precipitation variability in kumaon Himalaya, India over a perspective of ~ 300 years. *Quat. Int.* 325, 219–225. <https://doi.org/10.1016/j.quaint.2013.09.005>.